Online Learning-Enhanced High Order Adaptive Safety Control

Lishuo Pan¹, Mattia Catellani², Thales C. Silva¹, Lorenzo Sabattini², Nora Ayanian¹ Brown University, ²University of Modena and Reggio Emilia

Abstract—Control barrier functions (CBFs) are an effective model-based tool to formally certify the safety of a system. With the growing complexity of modern control problems, CBFs have received increasing attention in both optimization-based and learning-based control communities as a safety filter, owing to their provable guarantees. However, success in transferring these guarantees to real-world systems is critically tied to model accuracy. For example, payloads or wind disturbances can significantly influence the dynamics of an aerial vehicle and invalidate the safety guarantee. In this work, we propose an efficient vet flexible online learning-enhanced high-order adaptive control barrier function using Neural ODEs. Our approach improves the safety of a CBF-certified system on the fly, even under complex time-varying model perturbations. In particular, we deploy our hybrid adaptive CBF controller on a 38g nano quadrotor, keeping a safe distance from the obstacle, against 18km/h wind.

I. INTRODUCTION

As the complexity of both robotic mechanical systems and tasks increases, such as high-dimensional, nonlinear systems and agile control in quadrotors or quadruped robots, it leads to a broader adoption of learning-based approaches, which often come without safety guarantees. This necessitates rigorous safety guarantees built into the controller by definition. Control barrier functions (CBFs) have become a popular model-based tool for safety-critical control owing to their formal guarantees on set invariance (i.e., safety) without compromising performance [1], [2]. The CBF approach generates safe control for a closed-loop system by solving a quadratic program (QP). In practice, however, CBF-certified systems can sometimes fail to meet safety requirements because of an inaccurate model. This inaccuracy is often caused by a model mismatch or by external forces, like changes in payload or wind disturbances. The adaptive CBFs (aCBFs) compensate for complex dynamic residuals and improve safety in real-world systems, serving as a viable solution for the aforementioned potential safety violations.

Inspired by the recent success of data-driven approaches that learn the model of complex dynamical systems [3]–[5], we propose a learning-enhanced high-order adaptive CBF (HO-aCBF) that improves safety performance online, handling time-varying model perturbations. Our hybrid approach combines a nominal model with a neural network residual model to efficiently estimate the true dynamics using Knowledge-based Neural ODEs [4] that obey physical laws. The model trains on state-control observations and allows data to be sampled with different time intervals (typical for a real-time system). Our hybrid model approach offers high data efficiency compared to a pure learning-based approach by utilizing a nominal model, yet has the rich expressiveness of a neural network to capture complex residuals on the fly.



Fig. 1: A 38g nano quadrotor tracks a circular trajectory while keeping a safe distance from the obstacle, against an 18km/h wind. The safety is improved on-the-fly, i.e., the quadrotor moves further away from the obstacle after experiencing the wind once.

Recently, studies have shown that aCBFs (specifically, residual learning approaches) are effective in improving the safety of a system under model perturbations [6], [7]. However, these methods require offline training and online deployment, which leads to safety violations when the residuals have never been seen before (i.e., they are out of the training distribution). In contrast, our learning-enhanced aCBF, owing to its hybrid model approach, can efficiently adapt to unseen residuals online, making it well-suited for real-world systems. In addition, in [6], [7], supervision of time derivatives of a control barrier function is required, which is often obtained from noisy numerical differentiations. Instead, we use the Neural ODEs to approximate the residual dynamics directly from observable state-control data. In practice, most CBF constraints for a mechanical system have relative degrees larger than one, thus requiring a high-order CBF (HOCBF). Our HO-aCBF algorithm generalizes the standard aCBF to handle high-order safety-critical constraints for a larger category of systems.

There exist robust CBF methods that guarantee safety against model perturbations, where safety is achieved by adding a robustifying term in CBF constraints [8]. Robust CBFs, however, require knowing the bounds of the model uncertainty (usually unknown in practice) and result in overly conservative controllers. Recently, robust adaptive CBFs (RaCBFs) have been proposed [9]–[11]. In their formulation, an aCBF is used to mitigate over-conservativeness by estimating parametric uncertainty. The authors in [12] extend the concurrent-learning aCBFs in [13] to HO-aCBFs. In these works, a strong assumption is made that the residual is a linear model combining a known knowledge matrix and a learnable constant vector. In many practical cases, this matrix may not be available, and the uncertainty is not constant, thus breaking their theoretical safety guarantees. Extensive gain tuning is

also necessary for the concurrent-learning HO-aCBF method, requiring a specialist on-site.

Unlike aCBF frameworks in [9]–[13], our approach requires no prior knowledge of residual dynamics, captures unknown complex time-varying dynamics, and is robust to controller tuning. In our experiments, we demonstrate that HO-aCBF approaches that estimate residual dynamics using a linear model are ineffective in utilizing the long-term state-control data to extract residual patterns, resulting in inadequate performance when handling time-varying residuals. Additionally, our hybrid approach improves data efficiency compared to residual learning approaches in [6], [7], making it suitable for online adaptation. These learning frameworks [6], [7] require estimating time derivatives of a control barrier function using numerical differentiation. Instead, our approach learns the residual dynamics directly from state-control data.

The contributions of this work are twofold:

- a learning-enhanced high-order adaptive CBF that improves safety under complex time-varying model perturbations; and
- an online hybrid approach using Knowledge-based Neural ODEs that solves CBF optimization with learnable parameters at 100Hz and trains online.

We demonstrate our controller's efficacy in simulation with different types of nonstationary residuals, benchmarked with baseline HOCBFs [14], HO-aCBFs [12], [13] (with different hyperparameters). In physical experiments, we deploy our algorithm on a nano quadrotor weighing only 38g against $18 \mathrm{km/h}$ turbulent wind and efficiently improve safety performance on the fly.

II. PRELIMINARIES

A. High-order Control Barrier Functions (HOCBFs)

Consider a nonlinear control affine system in the form

$$\dot{\mathbf{x}} = f(\mathbf{x}) + g(\mathbf{x})\mathbf{u},\tag{1}$$

where $f: \mathbb{R}^p \to \mathbb{R}^p$ and $g: \mathbb{R}^p \to \mathbb{R}^{p \times q}$ are Lipschitz continuous functions, and $\mathbf{u} \in U \subset \mathbb{R}^q$ is the control input. A closed set $\mathcal{C} \in \mathbb{R}^p$ is forward invariant for the closed-loop system $\dot{\mathbf{x}}$ if $\mathbf{x}(0) \in \mathcal{C} \Rightarrow \mathbf{x}(t) \in \mathcal{C}, \forall t$. In this paper, the forward invariance property is used to formally define the notion of "safety". It is assumed that any safe set can be expressed as a zero-superlevel set of a continuously differentiable function $h(\mathbf{x}): \mathbb{R}^p \to \mathbb{R}$, written as

$$C = \{ \mathbf{x} \in \mathbb{R}^p \mid h(\mathbf{x}) \ge 0 \}. \tag{2}$$

A control barrier function is a popular tool to produce controls that render the set (2) forward invariant for (1). Classical (order-one) CBF formulations, however, are conditioned on the assumption that h has relative degree one with respect to (1).

Definition 1 (Relative degree [15]). A sufficiently smooth function h is said to have *relative degree* $r \in \mathbb{N}$ with respect to (1) on the set \mathbb{R}^p if 1) $L_g L_f^{i-1} h(\mathbf{x}) = 0$, for all $1 \le i \le r-1$, and 2) $L_g L_f^{r-1} h(\mathbf{x}) \ne 0$ for all $\mathbf{x} \in \mathbb{R}^p$.

For most mechanical systems and their safety requirements, h, a higher relative degree is required. High-order control barrier functions provide safety for such systems.

Definition 2 (HOCBFs [14], [16]). Consider a system as in (1). Let $\{C_i\}_{i=1}^r$ be a collection of sets of the form $C_i = \{\mathbf{x} \in \mathbb{R}^p \mid \psi_{i-1} \geq 0\}$ satisfying

$$\psi_r(\mathbf{x}) = \dot{\psi}_{r-1}(\mathbf{x}) + \alpha_r(\psi_{r-1}(\mathbf{x})) \tag{3}$$

$$\psi_0(\mathbf{x}) = h(\mathbf{x}),\tag{4}$$

where $\{\alpha_i\}_{i=1}^r$ is a set of differentiable extended class \mathcal{K} functions. A function h is said to be a HOCBF of order r for (1) on an open set $\mathcal{D} \supset \cap_{i=1}^r \mathcal{C}_i$ if h has relative degree r on some nonempty $\mathcal{R} \subseteq \mathcal{D}$ and there exists a suitable choice of $\{\alpha_i\}_{i=1}^r$, such that for all $x \in \mathcal{D}$

$$\sup_{\mathbf{u}\in U}\left[\underbrace{L_f\psi_{r-1}(\mathbf{x}) + L_g\psi_{r-1}(\mathbf{x})\mathbf{u} + \alpha_r(\psi_{r-1}(\mathbf{x}))}_{\psi_r(\mathbf{x},\mathbf{u})}\right] \ge 0. \quad (5)$$

Theorem 1 ([16]). Let h be a HOCBF for (1) on $\mathcal{D} \subset \mathbb{R}^p$ as in Def. 2. Any locally Lipschitz controller $\mathbf{u} \in U$ that satisfies $\psi_r(\mathbf{x}, \mathbf{u}) \geq 0$, renders $\bigcap_{i=1}^r \mathcal{C}_i$ forward invariant for the closed-loop system as in (1).

B. Knowledge-based Neural ODEs (KNODE)

KNODE [4] is an efficient data-driven approach that approximates a dynamical system relying on state-control pairs, i.e., $\mathbf{z} := [\mathbf{x}; \mathbf{u}]$. Its efficiency comes from combining a nominal model (typical for a mechanical system) with a neural network, learning merely the residual dynamics. The hybrid model is given by

$$\dot{\mathbf{x}} = \tilde{f}(\mathbf{z}) + \hat{f}_{\theta}(\mathbf{z}) = f_h(\mathbf{z}, \hat{f}_{\theta}(\mathbf{z})), \tag{6}$$

where \tilde{f} denotes a nominal model and \hat{f}_{θ} denotes the residual model estimated by a neural network parameterized with θ . The neural ODE-based approach learns the model of a dynamical system. Instead of learning in the state space, it learns its dynamical model directly and predicts the state using ODE solvers, thus allowing observations sampled with different time intervals (typical in a physical real-time system). An efficient learning approach preserves the physics of a dynamic model, making it well-suited for our online HO-aCBF controller.

III. PROBLEM FORMULATION

Consider a robot that follows a reference trajectory with a desired control $\mathbf{u}_{\mathrm{des}}$ and avoids obstacles by certifying the desired control using a CBF with unknown dynamic perturbations. The guarantee provided by CBF can be compromised due to the inaccurate model. We adopt the formulation in [9], and assume the true dynamics in the following form

$$\dot{\mathbf{x}} = f(\mathbf{x}) + g(\mathbf{x})\mathbf{u} + d(\mathbf{x}),\tag{7}$$

where $f(\mathbf{x}) + g(\mathbf{x})\mathbf{u}$ forms a nominal model and $d(\mathbf{x})$ includes all unmodeled model residuals and is allowed to change over time. The problem we want to solve is to recover the safety guarantee of the CBF-based controller by identifying the complex model perturbation $d(\mathbf{x})$ using online state and control data

We propose an efficient learning-enhanced high-order aCBF that compensates for unknown complex time-varying and nonlinear dynamic perturbations $d(\mathbf{x})$ and improves the system

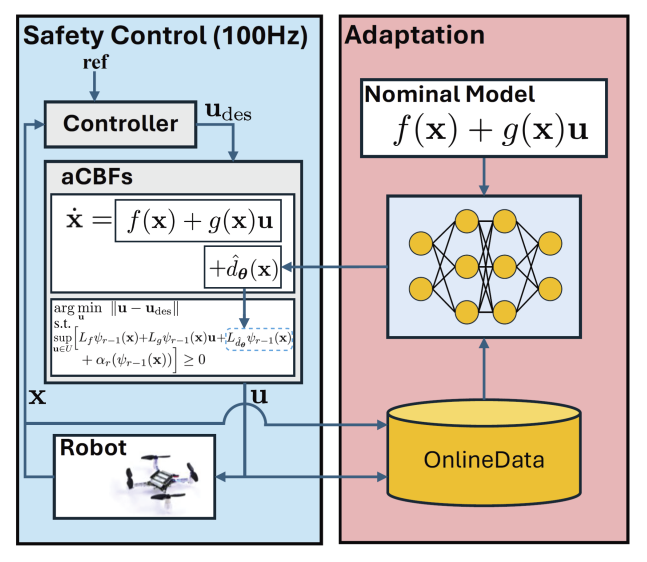


Fig. 2: The picture depicts the system overview of our NODE-HO-aCBF framework. The safety control solves the NODE-HO-aCBF QP, which uses the most recently trained model, at 100Hz to certify the desired control. The state and control input data are stored in an online queue for training. The hybrid adaptation module combines a nominal model with a learning-based term that approximates the unknown residual dynamics online.

safety performance online. Our hybrid model combines the nominal model with a neural network residual model \hat{d}_{θ} parameterized with θ , using Knowledge-based Neural ODEs [4] that obey physical laws. The residual model is trained on observable state-control data, i.e., $\mathbf{z} := [\mathbf{x}; \mathbf{u}]$. Furthermore, we generalize the proposed aCBFs to high-order aCBFs to handle a larger category of systems.

IV. LEARNING-ENHANCED HIGH-ORDER ADAPTIVE CONTROL BARRIER FUNCTIONS

CBF-based controllers are safe by definition for a known dynamical system. In practice, such safety guarantees can be violated due to model inaccuracies, such as not fully capturing the true dynamics of the robot. In this work, we propose an efficient learning-enhanced high-order aCBF using knowledge-based neural ODEs, or NODE-HO-aCBF for short. Our approach compensates for complex model perturbations from observable state-control data, improving safety on the fly. In Sec. IV-A, we introduce our learning-enhanced NODE-HO-aCBF optimization framework. In Sec. IV-B, we introduce KNODE for learning residual dynamics online. In Sec. V-A, we present an example of a double integrator that maintains a safety distance from obstacles using our NODE-HO-aCBF controller. The overall framework for NODE-HO-aCBF is depicted in Fig. 2.

A. Learning-enhanced HO-aCBFs

Simplified models are often chosen for their efficiency and analytical advantages in robotics applications. These models, however, do not capture the true dynamics. For example, a quadrotor cannot follow a double integrator trajectory precisely due to its kinematic constraints. Time-varying external residual dynamics, such as wind turbulence or downwash effect between quadrotors flying in close proximity, also introduce an unmodeled nonlinear term to the model. Our

approach enables a high-order adaptive CBF to learn such model mismatches and external dynamics from data, therefore, improving safety on the fly.

We assume the true dynamics as in (7), where we consider a time-varying model perturbation term $d(\mathbf{x})$, which depends on the robot state and is allowed to change over time. We formulate our hybrid model, combining the known nominal dynamics with a neural ODE approximated residual dynamics, as follows

$$f_h(\mathbf{z}, \hat{d}_{\theta}(\mathbf{x})) = f(\mathbf{x}) + g(\mathbf{x})\mathbf{u} + \hat{d}_{\theta}(\mathbf{x}),$$
 (8)

where \hat{d}_{θ} denotes the residual dynamics estimated by a neural network parameterized with θ .

As a model-based approach, successfully transferring its guarantee to real-world systems is inherently tied to the fidelity of the system model. To handle model perturbation, we consider the hybrid model from (8) and propose a Neural ODE enhanced high-order adaptive control barrier function, namely, NODE-HO-aCBF. Similar to a typical HOCBF QP formulation, the objective is to minimize the deviation between the safe control and the desired control input. To adapt to the unknown residual dynamics, we modify the HOCBF constraint in (5) to (9b). The Lie-derivative of residual term \hat{d}_{θ} , i.e., $L_{\hat{d}_{\theta}}$, is added to the HOCBF constraint to certify the hybrid system model. We formulate the QP for NODE-HO-aCBF as follows:

$$\arg\min \|\mathbf{u} - \mathbf{u}_{\mathrm{des}}\| \tag{9a}$$

s.t.
$$\sup_{\mathbf{u}\in U} \left[L_f \psi_{r-1}(\mathbf{x}) + L_g \psi_{r-1}(\mathbf{x}) \mathbf{u} + L_{\hat{d}_{\theta}} \psi_{r-1}(\mathbf{x}) \right]$$

$$+ \alpha_r(\psi_{r-1}(\mathbf{x})) \Big] \ge 0, \tag{9b}$$

where,

$$\psi_r = \dot{\psi}_{r-1} + \alpha_r(\psi_{r-1}) \tag{10}$$

$$= \left(\frac{\partial \psi_{r-1}}{\partial \mathbf{x}}\right)^{\top} \left(f + g\mathbf{u} + \hat{d}_{\boldsymbol{\theta}}\right) + \alpha_r(\psi_{r-1}) \tag{11}$$

$$\psi_0 = h(\mathbf{x}). \tag{12}$$

To compute ψ_r , the algorithm requires taking the (r-1)-th derivative of the residual dynamics $\hat{d}_{\boldsymbol{\theta}}$ estimated by the neural network w.r.t. the state, i.e. $\nabla_{\mathbf{x}}^{r-1}\hat{d}_{\boldsymbol{\theta}}$, which can be computed by automatic differentiation from machine learning frameworks or numerical methods. Our learning-enhanced controller runs at $100 \mathrm{Hz}$ to provide high-frequency safety control for the real-time system. At each iteration step (see Algo. 1), the NODE-HO-aCBF loads the hybrid model if a new learned model is ready. A PID controller takes the current state \mathbf{x} and reference $\mathbf{x}_{\mathrm{ref}}$ to generate a desired control $\mathbf{u}_{\mathrm{des}}$. By solving the QP in (9), a safe control \mathbf{u} is produced and executed by the robot. The state-control pair $\mathbf{z} := [\mathbf{x}, \mathbf{u}]$ is added to the online queue for training.

B. KNODE Online Learning

An unknown nonstationary residual, as prior models quickly become obsolete, requires continuous online adaptation to identify the current true dynamics on the fly.We employ a

Algorithm 1: Learning-enhanced HO-aCBF Control Loop

Initialize the current time, latest model update time, total duration and training data as t_i, t_m, t_T , and $\mathcal{Q}_{\text{train}}$ 2 $t_i \leftarrow 0$; $\mathcal{Q}_{\text{train}} \leftarrow [\]$ 3 while $t_i < t_T$ do
4 | if New hybrid model is available then
5 | NODE-HO-aCBF loads the new model
6 | PID generate a desired control \mathbf{u}_{des} given robot state \mathbf{x} and a reference \mathbf{x}_{ref} 7 | Solve QP in (9) and generate a safe control \mathbf{u} 8 | Robot updates the state using \mathbf{u} 9 | Append \mathbf{z}_{t_i} to the queue $\mathcal{Q}_{\text{train}}$ (pop out the oldest data if the queue is full).

 $t_i \leftarrow \text{current time}$

10

training queue $\mathcal{Q}_{\mathrm{train}}$ to store state-control pairs in a first-in, first-out (FIFO) manner, ensuring that the hybrid model f_h is trained online with the most recent data. The neural ODE learns a dynamical system directly. Consider an objective function \mathcal{L} that penalizes the error between the predictions and observations by constraining the prediction state to obey a learning-based ODE, defined as follows,

$$\mathcal{L}(\boldsymbol{\theta}) = \frac{1}{m-1} \sum_{i=1}^{m-1} \int_{t_i}^{t_{i+1}} \delta(t_s - \tau) \|\hat{\mathbf{x}}_{\tau} - \mathbf{x}_{\tau}\|^2 d\tau + \lambda \|\boldsymbol{\theta}\|_2^2$$
(13)

where m is the number of samples in $\mathcal{Q}_{\text{train}}$, $\delta(\cdot)$ is the Dirac delta function, t_s is any sampling time in $\mathcal{Q}_{\text{train}}$, \mathbf{x}_{τ} is a shorthand for $\mathbf{x}(\tau)$. For the learned model to generalize, we use the norm-2 regularization with a weight λ [17]. The prediction state is computed as follows:

$$\hat{\mathbf{x}}_{\tau} = \mathbf{x}_{t_i} + \int_{t_i}^{\tau} f_h(\mathbf{z}_w, \hat{d}_{\boldsymbol{\theta}}(\mathbf{x}_w)) dw. \tag{14}$$

The learnable parameters are obtained by solving the following optimization problem:

$$\underset{\boldsymbol{a}}{\operatorname{arg\,min}} \ \mathcal{L}(\boldsymbol{\theta}) \tag{15a}$$

s.t.
$$\dot{\mathbf{x}} = f_h(\mathbf{z}, \hat{d}_{\boldsymbol{\theta}}(\mathbf{x})).$$
 (15b)

In practice, a gradient-based optimization tool, such as Py-Torch, can be employed to solve the above optimization problem efficiently.

Our algorithm can also be used in offline mode. In offline mode, we collect state-control data by operating the vehicle using the HOCBF safety controller for a certain duration. We pre-train the neural network to approximate the residual dynamics using all the data collected and deploy the NODE-HO-aCBF controller with the learned $\hat{d}_{\theta}(\mathbf{x})$.

V. SIMULATIONS

To demonstrate the efficacy of the proposed algorithm, we apply it in a simulation with a double integrator model with different types of model residuals.

Algorithm 2: Online Dynamic Learning

```
1 Initialize the current time, total duration, training data as t_i, t_T, \mathcal{Q}_{\text{train}}, and the hybrid model in (8)

2 while t_i < t_T do

3 | if \mathcal{Q}_{\text{train}} \neq \emptyset then

4 | Train the hybrid model by optimizing (15) using \mathcal{Q}_{\text{train}}

5 | Save the new model

6 | t_i \leftarrow current time
```

A. NODE-HO-CBFs with Double Integrator Nominal Model

We consider an example where a robot is required to follow a reference trajectory in a workspace containing obstacles $\mathcal{O}_1,\ldots,\mathcal{O}_{N_{\mathrm{obs}}}$, from which the robot is required to keep a safety distance D_s . The robot state $\mathbf{x}=[\mathbf{r};\dot{\mathbf{r}}]\in\mathbb{R}^6$ represents its position and velocity. The control input $\mathbf{u}\in\mathbb{R}^3$ is the acceleration. We consider the nominal model as a double integrator, and the hybrid model can be written

$$\dot{\mathbf{x}} = A\mathbf{x} + B\mathbf{u} + \hat{d}_{\boldsymbol{\theta}}(\mathbf{x}),\tag{16}$$

where $A = [\mathbf{0}, \mathbf{I}; \mathbf{0}, \mathbf{0}] \in \mathbb{R}^{6 \times 6}$, $B = [\mathbf{0}; \mathbf{I}] \in \mathbb{R}^{6 \times 3}$. Here $\mathbf{0} \in \mathbb{R}^{3 \times 3}$, $\mathbf{I} \in \mathbb{R}^{3 \times 3}$ are the zero and identity matrices, respectively.

At each iteration step, we obtain a reference of position, velocity, and acceleration, i.e., $[\mathbf{r}_{\mathrm{des}}; \mathbf{v}_{\mathrm{des}}; \mathbf{a}_{\mathrm{des}}]$. The desired control $\mathbf{u}_{\mathrm{des}}$ is generated using a PID controller. We investigate the CBF that ensures safety by maintaining a minimum distance from obstacles. Specifically, we define the CBF corresponding to the i-th obstacle as

$$h_i(\mathbf{x}) = \|\mathbf{r} - \mathbf{r}_{\text{obs},i}\|_2^2 - D_s^2, \forall i \in \{1, \dots N_{obs}\},$$
 (17)

where $\mathbf{r}_{\mathrm{obs},i}$ denotes the position of *i*-th obstacle. The relative degree of h_i is two with respect to the model in (16), according to Def. 1. We consider the extended class \mathcal{K} functions as $\alpha_i(h) = \gamma_i h$. Thus the optimization is formulated as follows:

The solution of the optimization (18) is the control ${\bf u}$ for our hybrid learning-enhanced high-order aCBF controller.

B. Simulation Setups

A perturbed double integrator is implemented as $\dot{\mathbf{x}} = A\mathbf{x} + B\mathbf{u} + d(\mathbf{x})$, where we assume the residual dynamics $d(\mathbf{x})$ is unknown to the robot in the simulation. Three types of residuals are considered, namely, "Attractive", "Repulsive", and "Time-varying". In "Attractive" and "Repulsive" experiments, residuals attract and repulse the robot towards and away from the center of a forbidden region where the robot is not allowed

to enter, i.e., $d_{\rm att}(\mathbf{x}) = [\mathbf{0}; -k\mathbf{r}], d_{\rm rep}(\mathbf{x}) = [\mathbf{0}; k\mathbf{r}],$ where k = 0.4. In "Time-varying" experiment, residuals change between repulsive and attractive over time, i.e., $d_{\rm var}(\mathbf{x}) = [\mathbf{0}, k\sin(t)\mathbf{r}],$ where k = 1.0. A Runge–Kutta (RK4) numerical solver with sampling time of $\Delta t = 0.01\mathrm{s}$ is used to simulate the system response given the control. A closed-loop PID controller synthesizes the desired closed-loop response $\mathbf{u}_{\rm des}$. We assume the robot state-control pair $\mathbf{z} := [\mathbf{x}; \mathbf{u}]$ is observable and can be measured at $100\mathrm{Hz}$. The closed-loop control is applied at a rate of $100\mathrm{Hz}$. We use a similar neural network architecture to [18]. The value of $\hat{d}_{\boldsymbol{\theta}}$ is computed as the addition of outputs of three parallel neural networks with the same architecture and input \mathbf{x} . Each neural network has two hidden layers, each with only 16 neurons, where the hyperbolic tangent activation function is applied after the first hidden layer.

The robot is commanded to follow a circular reference trajectory of radius $2\mathrm{m}$ at height $1\mathrm{m}$, centered at the x-y plane origin, where a spherical forbidden region of radius $D_s=3\mathrm{m}$ is also located. Thus, the CBF must be effective to avoid safety violations. Our NODE-HO-aCBF controller supports both offline and online modes as described in Sec. IV-B. For our online NODE-HO-aCBF controller, we maintain an FIFO queue of 10 seconds of online data for training. For the offline model, we collect 40 seconds of state-control data for training.

Benchmarking. We compare the safety performance between: 1) HOCBFs baseline [14] (we use the open-source implementation from [19]), where no external residual exists, 2) HOCBFs baseline, 3) HO-aCBFs baseline [12], [13], 4) our online NODE-HO-aCBFs, and 5) our offline NODE-HOaCBFs. The HOCBF controller without the external residual sets the baseline safety performance of the system. The comparison of online and offline NODE-HO-aCBFs with HOCBFs baseline demonstrates that our algorithm improves safety performance by adapting to the residual term. The comparison of online and offline NODE-HO-aCBFs with the adaptive HOCBFs highlights that our algorithm can handle time-varying residuals, and our algorithm does not require knowledge of the residual dynamics nor extensive tuning. For all the approaches, we use extended class \mathcal{K} functions $\alpha_i(h) =$ $\gamma_i h$, where $\gamma_i = 2$ for i = 1, 2, in CBF constraints. For the HO-aCBFs baseline [12], [13], it is assumed that $d(\mathbf{x}) =$ $Y(\mathbf{x})\hat{\boldsymbol{\vartheta}}$, where $Y(\mathbf{x}) \in \mathbb{R}^{p \times s}$ is a known matrix and $\hat{\boldsymbol{\vartheta}} \in \mathbb{R}^{s}$ is an unknown constant vector to estimate. To update the parameter ϑ , HO-aCBFs require computing its update law ϑ using an adaptation gain $\kappa \in \mathbb{R}_{>0}$ and a positive definite gain matrix $\Gamma \in \mathbb{R}^{s \times s}$ (see [12, eq. (14)]). We extensively tune the gains κ and Γ in their formulation of $\hat{\boldsymbol{\vartheta}}$ and assume a known $Y(\mathbf{x}) = [\mathbf{0}_{3\times3}; -r_1, 0, 0; 0, -r_2, 0; 0, 0, -(r_3 - 1)].$ Note that this is a strong assumption and we usually do not have prior knowledge about $Y(\mathbf{x})$ in practice. To compute the HO-aCBF controller online at 100Hz, we can only use a history stack of 0.5s. As we will point out in the following section, increasing the HO-aCBF's history stack does not improve its performance significantly, yet largely increases its runtime, prohibiting its performance. For HO-aCBF baseline [12], we set the bounds of the estimate ϑ between [-4, -4, -4] to [4, 4, 4], which sufficiently cover the range of the underlying dynamic residual

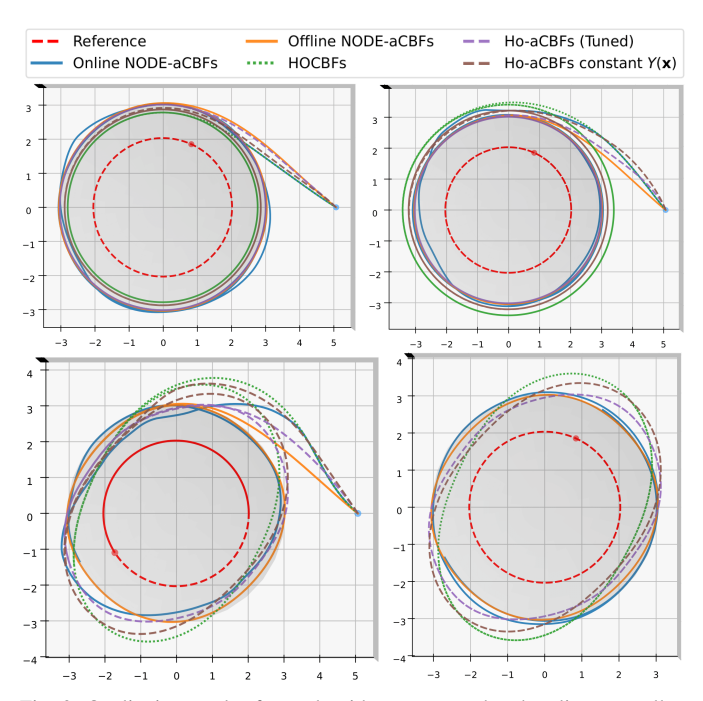


Fig. 3: Qualitative result of our algorithms compared to baseline controllers with the presence of external residual dynamics. The blue dot represents the initial state, and the red dot represents the current reference. The Gray sphere is the forbidden region. Top left: "Attractive" residual, Top right: "Repulsive" residual, Bottom left: "Time-varying" residual from 0-20s, Bottom right: "Time-varying" residual from 20-40s.

term given our choice of $Y(\mathbf{x})$ matrix.

C. Simulation Qualitative Results

We demonstrate the typical trajectories of baseline and our NODE-HO-aCBF controllers with three residual types in Fig. 3. In the "Attractive" experiment, the HOCBF baseline fails to adapt to external residuals, resulting in a significant safety violation and deviating from the safety boundary, as depicted by the green trajectory in the top-left panel. The HOaCBFs, when well-tuned and given a high-fidelity knowledge matrix $Y(\mathbf{x})$, are able to compensate for the residuals. When a constant matrix $Y(\mathbf{x})$ is applied, the HO-aCBF controller significantly violates safety and settles within the safety boundary, showcasing reduced adaptability, as indicated by the brown trajectory. Our approach, NODE-HO-aCBF, both its online and offline modes, are able to adapt to external residuals and settle safely outside of the forbidden region without tuning. In the "Repulsive" experiments, instead of being attracted towards the center and violating the safety, the baseline HOCBF controller settles farther from the center. The HO-aCBF baseline, similar to the "Attractive" experiment, is only able to adapt when a high-fidelity knowledge matrix is available and the controller is well-tuned. NODE-HOaCBFs, again, are able to adapt and settle at the boundary of the forbidden region. In both experiments, the residual term convergence rate of HO-aCBFs is higher than that of NODE-HO-aCBFs. However, due to the limitation on expressiveness of HO-aCBF, it is not practical for real-world systems under complex residual dynamics. We highlight NODE-HO-aCBFs' adaptive performance in the "Time-varying" experiment, as all baselines fail to adapt, even a well-tuned HO-aCBF controller. In the following analysis, we note that, even with an increased

Residual Type	Attractive				Repulsive				Time-varying						
Method	h_{\min}	h_{neg}	Avg.Dist.	Avg.sDist.	S.sDist.Var.	h_{\min}	h_{neg}	Avg.Dist.	Avg.sDist.	S.sDist.Var.	h_{\min}	h_{neg}	Avg.Dist.	Avg.sDist.	S.sDist.Var.
HOCBF - No residual	0.09	0.0%	0.07	0.01	2.02e-10	0.09	0.0%	0.07	0.01	2.02e-10	0.09	0.0%	0.07	0.01	2.02e-10
HOCBFs	-1.42	95.8%	0.27	0.25	8.20e-11	2.34	0.0%	0.42	0.37	5.64e-10	-2.78	44.7%	0.45	0.39	0.18
HO-aCBFs (Tuned)	-0.12	93.0%	0.06	0.01	9.89e-6	-0.10	89.5%	0.07	0.01	9.89e-6	-1.98	49.7%	0.27	0.23	0.06
HO-aCBFs $\Gamma = 1$	-1.50	92.6%	0.19	0.15	1.63e-3	13.31	0.0%	1.49e+9	2.97e+9	4.69e+19	-6.98	0.0%	1.47e+6	2.94e+6	3.74e+13
HO-aCBFs const $Y(\mathbf{x})$	-0.93	95.1%	0.19	0.16	1.44e-6	0.84	0.0%	0.24	0.18	5.29e-6	-2.65	45.4%	0.41	0.36	0.16
Online NODE-HO-aCBFs	-0.87	46.8%	0.07	0.02	3.93e-4	-1.61	37.7%	0.13	0.03	9.74e-4	-2.98	52.3%	0.20	0.04	2.29e-3
Offline NODE-HO-aCBFs	0.01	0.0%	0.06	0.01	1.45e-5	0.01	0.0%	0.06	0.01	1.62e-5	-0.91	68.5%	0.10	0.05	3.11e-3

TABLE I: h_{\min} , h_{neg} , Avg.Dist., Avg.sDist. and S.sDist.Var. metrics of the baseline controllers and our controllers with different types of residual dynamics. The statistics are averaged across 10 trials.

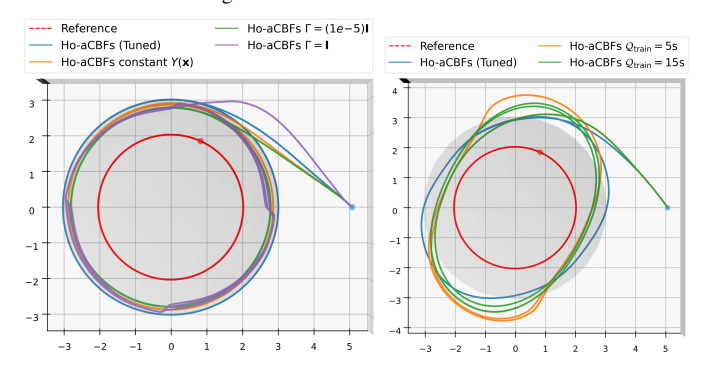


Fig. 4: Qualitative comparison between baseline HO-aCBF controller with different settings. "Attractive" residual (on the left), and "Time-varying" residual (on the right) are applied in experiments.

history stack for the HO-aCBF baseline, it cannot adapt to such a time-varying residual, but invalidates the desired control frequency and its real-time performance as its runtime grows with the history stack. Both our online and offline controllers can adapt and have significant advantages in settling closer to the safety boundary, i.e., improve the safety.

Next, we discuss tuning fragility, strong dependence on assumptions, and limited expressiveness of the HO-aCBF baseline. We tune the gains κ and Γ in the HO-aCBF controller, and provide a strong assumption of the knowledge matrix $Y(\mathbf{x})$. In Fig. 4 (left), the controller is executed in the "Attractive" experiment. Note that a small $\Gamma = (1e-5)\mathbf{I}$, a large $\Gamma = \mathbf{I}$, or a constant matrix $Y(\mathbf{x}) = [\mathbf{0}_{3\times 3}; -\mathbf{I}_{3\times 3}]$ (no knowledge) all lead to a quickly degenerated performance of the HOaCBF controller and result in significant safety violations. In Fig. 4 (right), we use the tuned HO-aCBF controller and increase its history stack Q_{train} to 5s and 15s (a long history stack invalidates the desired control frequency, so we freeze the simulation when computing the control). However, the controller cannot utilize the long history and still presents significant safety violations. These prominent drawbacks fragility to gains tuning, reliance on strong knowledge, and limited expressiveness in recognizing the pattern of a long horizon history stack-make it secondary compared to our approach when exposed to time-varying model perturbations.

D. Simulation Quantitative Results

We use the following quantitative evaluation criteria:

- h_{\min} : the minimum value of $h(\mathbf{x})$ during execution.
- h_{neg} : the fractional time for which $h(\mathbf{x}) < 0$ over execution time.
- Average Distance (Avg.Dist.): the average distance to the forbidden region surface over execution time.
- Average settleDistance (Avg.sDist.): same as Avg.Dist., excluding the first 20s in the simulation execution.
- Signed settleDistance Variance (S.sDist.Var.): the variance of the signed distance to the forbidden region

surface (negative value indicates the robot is inside the forbidden region), excluding the first 20s in the simulation execution.

In Table I, we record the averaged quantitative results from 10 simulation trials. In "Attractive" and "Repulsive" experiments, we observe that HO-aCBFs (Tuned), online NODE-HO-aCBFs, and offline NODE-HO-aCBFs are able to maintain a small Avg.Dist. and Avg.sDist., indicating their success in residual adaptation and safety improvement. However, the HOaCBF has high h_{neg} , indicating that the HO-aCBF controller failed to estimate a high-fidelity residual term to fully recover the safety. Among them, the offline NODE-HO-aCBF has the h_{\min} closest to that of HOCBF with no external residuals and 0% of h_{neg} , indicating the highest fidelity of residual estimations. These three controllers all demonstrate small S.sDist. Var., indicating their settled trajectory maintains a stable distance to the forbidden region surface. All other baselines fail to adapt in the "Attractive" and "Repulsive" experiments. In the "Time-varying" experiments, only our NODE-HO-aCBFs can adapt. According to Avg. Dist. and Avg.sDist. metrics, both online and offline NODE-HO-aCBFs are significantly closer to the safety boundary and have similar results with HOCBF with no external residuals. According to S.sDist.Var., our online and offline NODE-HO-aCBFs settle on trajectories that variate least from the safety boundary, indicating a stable adaptation. Note that even a well-tuned HO-aCBF controller results in large Avg.Dist., Avg.sDist. and S.sDist.Var., as depicted in Fig. 3 (bottom right). Offline NODE-HO-aCBFs learn offline and thus adapt the residual without delay, resulting in minimal h_{\min} . Online NODE-HOaCBFs have a learning delay, resulting in a slightly larger h_{\min} and Avg. Dist. than the offline method, but as it learns online, it adapts better and settles stabler with incoming data and results in a smaller Avg.sDist. and S.sDist.Var.

VI. PHYSICAL EXPERIMENTS

A. Physical Experiment Setup

The Crazyflie 2.1 nano quadrotor is used as the physical platform to verify the efficacy of our hybrid controller. The open-source library Crazyswarm [20] is used as an interface to send position-velocity-acceleration controls. The nano quadrotor weighs 38g with a 300mAh battery. A tower fan is placed horizontally at a height of 0.7m and 1.16m in the positive direction of the x-axis from the origin. Its horizontal airflow produces an effective turbulent region of approximately 0.55m wide, which travels 18km/h (its location and direction are depicted in Fig. 5). The quadrotor is required to keep a 1m distance from the origin. A laptop with Intel i7 is used as the base station, and communication with the Crazyflie is established using Crazyradio PA. We obtain 100Hz position

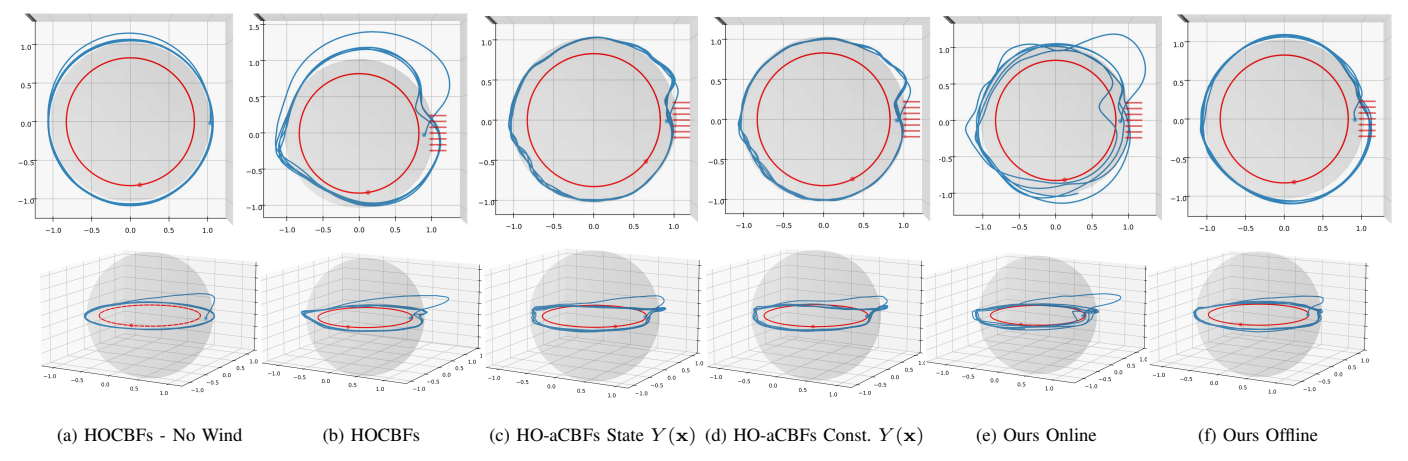


Fig. 5: The top views (first row) and the side views (second row) of 60s trajectories using different safety controllers in the physical experiments. The red arrows indicate the location and direction of the wind.

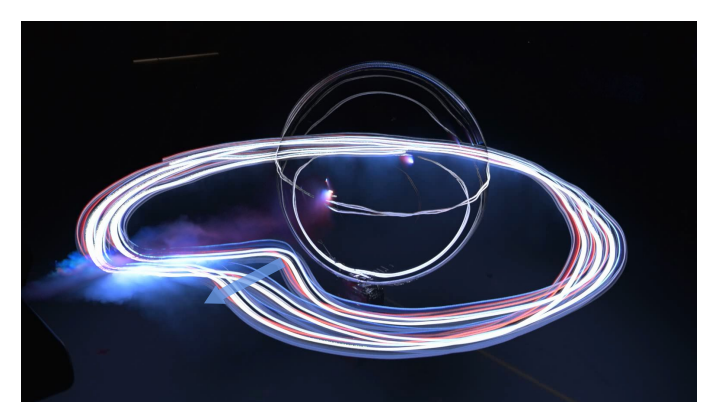


Fig. 6: Long exposure trajectory of the nano quadrotor, maintain the safety under wind turbulence. The blue arrow indicates the robot recovers safety over time.

data from VICON motion capture, and estimate velocity from filtering. Control inputs are computed and sent to the quadrotor at 100Hz. We increase the number of neurons in each layer to 64 in our NODE-HO-aCBF controller to capture the wind turbulence. We experiment with both online and offline modes of our NODE-HO-aCBF controller. For the offline mode, we trained on 350s state-control data collected by executing the HOCBF baseline controller. A representative physical experiment using our online NODE-HO-aCBF controller is shown in Fig. 6. Note that safety is improved against the wind on the fly. For the HO-aCBF baseline controller, we used the state-informed matrix $Y(\mathbf{x}) = [\mathbf{0}_{3\times3}; r_1, 0, 0; 0, r_2, 0; 0, 0, r_3]$, namely HO-aCBF State $Y(\mathbf{x})$, and a constant matrix $Y(\mathbf{x}) = [\mathbf{0}_{3\times3}; \mathbf{I}_{3\times3}]$, namely HO-aCBF Constant $Y(\mathbf{x})$.

B. Physical Experiment Results

We evaluate the efficacy of our controller both qualitatively and quantitatively. In Fig. 5, the first 60s of a representative trajectory for each controller is depicted as the blue curve; the gray area is the forbidden region; the red circle is the reference trajectory; and the red arrows indicate the wind location and direction. Notice that all the baseline methods (Fig. 5(b)-(d)) cannot handle the wind turbulence, and converged to an unsafe trajectory. Our online controller is able to improve safety after a few experiences with wind turbulence, while our offline controller, having learned the residuals, is able to significantly

improve safety at the beginning and maintain it throughout execution.

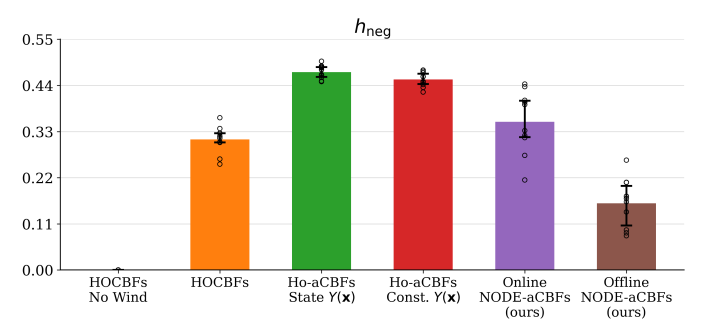
Table II and Fig. 7 show the quantitative results in the physical experiments. For the metrics computed on settled trajectory, i.e., Avg. sDist. and S. sDist. Var., we exclude the first 60s of the trajectory. The learning model takes longer to converge due to the sparsity of turbulence data. To highlight the adaptation results, we evaluate the trajectory segments where the wind causes significant effects, that is, from $[0, \pi/4]$, and $[\pi, 5\pi/4]$ radian on the x-y plane. Our offline approach results in fewer safety violations, as indicated by a smaller h_{neg} , adapts better to turbulence, according to smaller Avg.Dist. and Avg.sDist., and settled on a more stable trajectory, according to a smaller S.sDist.Var., compared to HOCBF and HO-aCBF baseline controllers. Note that our offline approach results in smaller Avg. Dist. and Avg. sDist. even compared to the HOCBF without wind turbulence, as model mismatches exist between a double integrator and a quadrotor model in the HOCBF controller, learning the residuals adapt to such model mismatch. Our online approach has a smaller $h_{\rm neg}$ than the HO-aCBF controller and is slightly larger than that of HOCBF, as the online approach requires sufficient data to learn the residual. As the online approach sees more data, it adapts turbulence better and settles on a more stable trajectory, as indicated by smaller Avg.sDist. and S.sDist. Var., compared to HOCBF and HO-aCBF controllers.

Method	h_{\min}	h_{neg}	Avg.Dist.	Avg.sDist.	S.sDist.Var.
HOCBFs - No Wind	0.03	0.0%	6.46e-2	6.39e-2	1.02e-4
HOCBFs	-0.34	31.1%	9.03e-2	8.30e-2	7.61e-3
HO-aCBFs position $Y(\mathbf{x})$	-0.23	47.2%	4.68e-2	4.76e-2	3.26e-3
HO-aCBFs const $Y(\mathbf{x})$	-0.22	45.4%	4.49e-2	4.53e-2	2.90e-3
Online NODE-HO-aCBFs	-0.55	35.3%	7.08e-2	4.29e-2	2.49e-3
Offline NODE-HO-aCBFs	-0.24	15.9%	4.44e-2	4.17e-2	1.34e-3

TABLE II: h_{\min} , h_{neg} , Avg.Dist., Avg.sDist. and S.sDist.Var. metrics of the baseline controllers and our controllers in the physical experiments. The statistics are averaged across 10 trials.

VII. CONCLUSION

In this work, we present a learning-enhanced high-order adaptive control barrier function that improves safety online under time-varying complex model perturbations. We use a hybrid structure that combines a nominal model with a neural network residual model, using neural ODEs. Due to its hybrid



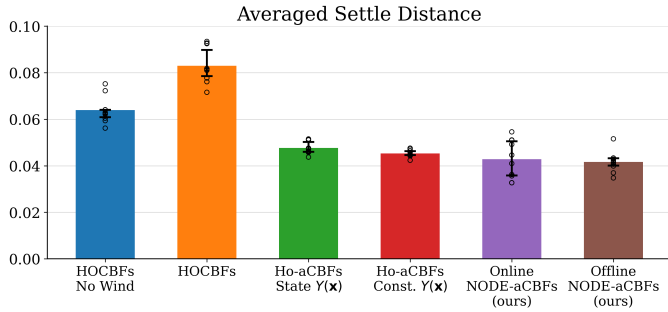


Fig. 7: $h_{\rm neg}$ and Avg.sDist. of baselines and our controllers. The top of the bars denotes the median, while the ends of the error bars represent the $25^{\rm th}$ and $75^{\rm th}$ percentiles. The statistics are obtained from 10 trials.

design, our controller is data-efficient and expressive, making it suitable for adapting complex, time-varying residuals online. We demonstrate its efficacy across three types of residuals in simulations and a representative physical experiment, benchmarked with baseline HOCBFs [14] and HO-aCBFs [12], [13] (with different hyperparameters). A 38g nano quadrotor, deployed with our online NODE-HO-aCBF controller, can quickly improve its safety performance in 18km/h turbulent wind. Current large-scale swarm trajectory planning algorithms, such as [21], [22], lack an adaptive controller that improves safety and stability in close-proximity flight. For future work, we aim to provide probabilistic safety guarantees for the controller proposed in this work and to improve the safety and stability of close-proximity trajectory planning for large-scale swarms.

REFERENCES

- [1] A. D. Ames, J. W. Grizzle, and P. Tabuada, "Control barrier function based quadratic programs with application to adaptive cruise control," in 53rd IEEE conference on decision and control. IEEE, 2014, pp. 6271–6278.
- [2] A. D. Ames, S. Coogan, M. Egerstedt, G. Notomista, K. Sreenath, and P. Tabuada, "Control barrier functions: Theory and applications," in 2019 18th European control conference (ECC). IEEE, 2019, pp. 3420–3431.
- [3] R. T. Chen, Y. Rubanova, J. Bettencourt, and D. K. Duvenaud, "Neural ordinary differential equations," Advances in neural information processing systems, vol. 31, 2018.
- [4] T. Z. Jiahao, M. A. Hsieh, and E. Forgoston, "Knowledge-based learning of nonlinear dynamics and chaos," *Chaos: An Interdisciplinary Journal* of Nonlinear Science, vol. 31, no. 11, 2021.
- [5] T. Z. Jiahao, L. Pan, and M. A. Hsieh, "Learning to swarm with knowledge-based neural ordinary differential equations," in 2022 International conference on robotics and automation (ICRA). IEEE, 2022, pp. 6912–6918.
- [6] A. Taylor, A. Singletary, Y. Yue, and A. Ames, "Learning for safety-critical control with control barrier functions," in *Learning for dynamics and control*. PMLR, 2020, pp. 708–717.
- [7] J. Choi, F. Castaneda, C. J. Tomlin, and K. Sreenath, "Reinforcement learning for safety-critical control under model uncertainty, using control lyapunov functions and control barrier functions," arXiv preprint arXiv:2004.07584, 2020.

- [8] M. Jankovic, "Robust control barrier functions for constrained stabilization of nonlinear systems," *Automatica*, vol. 96, pp. 359–367, 2018.
- [9] A. J. Taylor and A. D. Ames, "Adaptive safety with control barrier functions," in 2020 American Control Conference (ACC). IEEE, 2020, pp. 1399–1405.
- [10] B. T. Lopez, J.-J. E. Slotine, and J. P. How, "Robust adaptive control barrier functions: An adaptive and data-driven approach to safety," *IEEE Control Systems Letters*, vol. 5, no. 3, pp. 1031–1036, 2020.
- [11] M. Black and D. Panagou, "Safe control design for unknown nonlinear systems with koopman-based fixed-time identification," *IFAC-PapersOnLine*, vol. 56, no. 2, pp. 11369–11376, 2023.
- [12] M. H. Cohen and C. Belta, "High order robust adaptive control barrier functions and exponentially stabilizing adaptive control lyapunov functions," in 2022 American Control Conference (ACC). IEEE, 2022, pp. 2233–2238
- [13] A. Isaly, O. S. Patil, R. G. Sanfelice, and W. E. Dixon, "Adaptive safety with multiple barrier functions using integral concurrent learning," in 2021 American Control Conference (ACC). IEEE, 2021, pp. 3719– 3724.
- [14] W. Xiao and C. Belta, "High-order control barrier functions," *IEEE Transactions on Automatic Control*, vol. 67, no. 7, pp. 3655–3662, 2021.
- [15] H. K. Khalil and J. W. Grizzle, *Nonlinear systems*. Prentice hall Upper Saddle River, NJ, 2002, vol. 3.
- [16] X. Tan, W. S. Cortez, and D. V. Dimarogonas, "High-order barrier functions: Robustness, safety, and performance-critical control," *IEEE Transactions on Automatic Control*, vol. 67, no. 6, pp. 3021–3028, 2021.
- [17] C. Zhang, S. Bengio, M. Hardt, B. Recht, and O. Vinyals, "Understanding deep learning requires rethinking generalization," arXiv preprint arXiv:1611.03530, 2016.
- [18] T. Z. Jiahao, K. Y. Chee, and M. A. Hsieh, "Online dynamics learning for predictive control with an application to aerial robots," in *Conference* on Robot Learning. PMLR, 2023, pp. 2251–2261.
- [19] L. Pan, M. Catellani, L. Sabattini, and N. Ayanian, "Robust trajectory generation and control for quadrotor motion planning with field-of-view control barrier certification," arXiv preprint arXiv:2502.01009, 2025.
- [20] J. A. Preiss, W. Honig, G. S. Sukhatme, and N. Ayanian, "Crazyswarm: A large nano-quadcopter swarm," in 2017 IEEE International Conference on Robotics and Automation (ICRA). IEEE, 2017, pp. 3299–3304.
- [21] L. Pan, Y. Wang, and N. Ayanian, "Hierarchical trajectory (re) planning for a large scale swarm," arXiv preprint arXiv:2501.16743, 2025.
- [22] C. E. Luis, M. Vukosavljev, and A. P. Schoellig, "Online trajectory generation with distributed model predictive control for multi-robot motion planning," *IEEE Robotics and Automation Letters*, vol. 5, no. 2, pp. 604–611, 2020.